Multiwavelength Focusing with the Sun as Gravitational Lens

April 25, 2006

Laurent Koechlin, Denis Serre, Gerald K. Skinner, Peter Von Ballmoos, Thomas Crouzil

Abstract

The light deviation caused by the gravitational potential in the vicinity of the sun could be used as a means of focussing radiation that cannot be focussed easily otherwise. The gravitational lens formed by the sun is not stigmatic, but does have the advantage of being achromatic and acts identically on all types of mass-less radiations. For a source at infinity, its geometrical characteristics present a "caustic" line starting at 550 astronomical units (UA) downstream from the sun. In a plane perpendicular to that caustic line, images of distant objects are formed.

The perturbations by the solar corona plasma will significantly blur electromagnetic radiation for wavelengths longer than those of the IR domain. At shorter wavelengths, for example the γ domain, the focussing process could lead to 10^9 amplification factors. In order to reach the regions where images are formed, long distance space missions are necessary. Once launched, missions of this type would be dedicated to a single field. Some possible targets are considered, such as Sagitarius A observed in X and γ rays.

In this paper we study the point spread function (PSF) of the sun as a gravitational lens, taking into account perturbations by the planets and the non sphericity of the sun. Taking into account additional sources of perturbation, we derive limits within which such observations could be possible.

1 Introduction

The deviation of electromagnetic radiation by the sun's mass is a consequence of general relativity. It was observed as the first experimental confirmation of that theory: by Eddington (Dyson et al. 1919) in the visible, and later with more precision in the radio domain (Fomalont et al. 1975).

Using the optical effects of General Relativity for astrophysical purposes is not a new idea: Einstein himself has published a paper entitled "Lens-like Action of a Star by the Deviation of Light in the Gravitational Field" (Einstein, 1936), and the idea of using the sun as a gravitational lens for detecting nebulae dates from 1937 (Zwicky, 1937).

A lot of observational and theoretical work has since been done on gravitational lensing. It concerns principally the effect of lenses on distant fields when one or more lensing objects is present along the line of sight. From the resulting deformations, conclusions are drawn either about the gravitational potential of the lensing objects, or about the distant source objects (detected thanks to gravitational intensification) or the environment of stellar objects through microlensing (Paczynski 1996).

In the case studied here, the situation is different: the distant field is not imaged by a telescope. The sun itself *is* the focussing telescope, acting as an optical lens. A detector placed at a large distance from the inner solar system scans a "focal plane" of that lens. The deformation of the far field that is usually studied around a gravitational lens is not imaged here. What is recorded is an image plane, where a non-distorted and strongly intensified image of a narrow distant field is formed.

In this paper we will study the geometry of the problem, the scales involved, and the relatively "tough to deal with" Point Spread Function (PSF) of an imaging system involving a spherical mass as focussing objective. We will define upper limits for the aberrations caused by the gravitational perturbations from solar system objects and the non sphericity of the sun.

Finally we will propose an observing scheme for a space mission dedicated to Sagitarius A in the 511 keV domain.

2 Geometry of the problem

In the "thin lens" approximation, the deviation angle caused to a ray approaching at a closest distance r (impact parameter) from a mass M is

$$\theta = 4GM/rc^2 \tag{1}$$

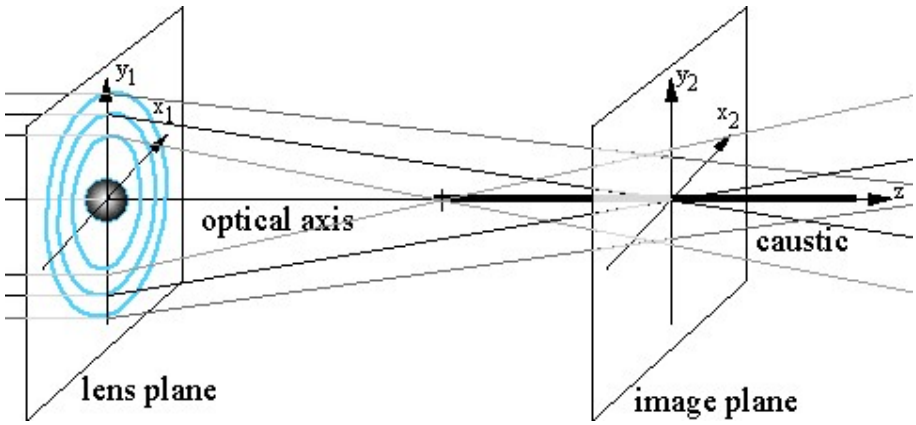

Figure 1: Position of the different planes and optical axis for the sun as a gravitational lens.

where $G = 6.676 \times 10^{-11} m^3\, kg^{-1}\, s^{-2}$ is the gravitation constant, and $c = 299792458\, m\, s^{-1}$ the speed of light.

In the case of light grazing the sun, where $M = m_\odot \simeq 1.989 \times 10^{30}$ kg and $r \geq r_\odot \simeq 6.96 \times 10^8$ m , the deviation angle is $\theta = 1.75$ arc seconds.

Using the small angles approximation, the shortest distance f at which originally parallel beams intersect when deflected by the sun is:

$$f = r^2 c^2 / 4GM, \tag{2}$$

The rays intersection locus (a caustic) is a line starting at a distance f after the lens end extending to infinity. For a one solar mass object and one solar radius impact parameter, the minimum "focal length" f is 548 astronomical units(AU) i.e. 8.2×10^{13}m. The impact parameter r may be smaller than a solar radius if one considers a transparent sun, as for neutrinos and gravitational waves (Macone 1999), leading to shorter starting points of the optical caustic: f can be as small as 40 AU : 5.98×10^{12}m. A non-zero neutrino mass will further shorten the focal length.

In the case of X and γ rays, the impact parameter will be in the range of 1.1 to 1.5 solar radius, leading to focal distances of hundreds of AU.

3 Point Spread Function of a "perfect" gravitational lens

From the strong dependence (eq. 2) of its "convergence length" f upon the impact parameter r, one can see that a gravitational lens is not stigmatic.

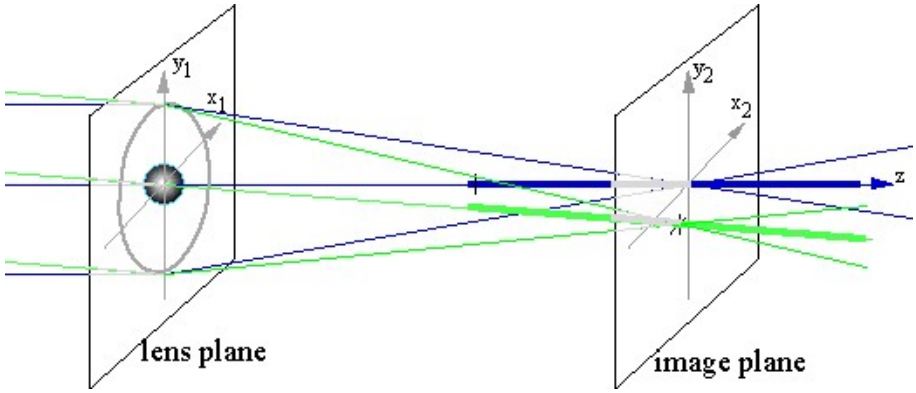

Figure 2: Images of two distant point sources represented as the intersection of their corresponding caustics and an image plane.

However, although a gravitational lens has no optical axis, no pupil plane and no focal plane, one can define arbitrarily an optical axis as the line from a point source passing through the lens's center of mass, a pupil plane (or lens plane) as a plane perpendicular to the optical axis and containing the center of mass, and finally a focal plane as a plane parallel to the pupil plane, at a distance from the center of mass corresponding to the convergence length f. As f varies according to r, a given focal plane is related to a given impact parameter for a source at infinity.

In the following, subscript "$_1$" indicates variables in the lens plane, and subscript "$_2$" variables in an arbitrarily chosen focal plane. We use polar coordinates (r, α) and consider an elemental area in each plane: $dS_1 = r_1 dr_1 d\alpha_1$ and $dS_2 = r_2 dr_2 d\alpha_2$.

The light from a point source is not actually focussed by a gravitational lens, but it is locally intensified in the vicinity of the caustic. One can define a Point Spread Function (PSF), from the expression of the intensification as a function of the position in the focal plane: $I(r_2, \alpha_2)/I_0$, I_0 being the "unfocussed" light intensity from the distant source if the focussing mass were not present.

The light collected by dS_1 in the lens plane is sent into the conjugate area dS_2 in the focal plane. $I(r_2)$ can be derived from the ratio dS_1/dS_2. High intensification occurs as dS_1 is much larger than dS_2.

$$I(r_1, r_2, \alpha_1, \alpha_2) = I_0 \frac{dS_1}{dS_2} = I_0 \frac{r_1 dr_1 d\alpha_1}{r_2 dr_2 d\alpha_2}. \tag{3}$$

To express I as a function of (r_2, α_2) only, we need relations between r_1, r_2, α_1 and α_2.

For the moment, we consider a centrosymetric mass distribution. This implies that $\alpha_1 = \alpha_2$, yielding a centro-symmetric PSF, which only depends on the distance r_2 from the caustic. The relation between r_2 and r_1 is given by

$$r_2 = r_1 - f\theta \ ,$$

which yields, after replacing f and θ by their expressions in eqs. (1) and (2):

$$r_2 = r_1 - {r_0}^2/r_1 \tag{4}$$

where r_0 is the radius of the "Einstein ring": the locus of points in the lens plane from which light intersections the caustic in that particular focal plane. r_1 can be expressed as a function of r_2:

$$r_1 = \frac{r_2 \pm \sqrt{4\,{r_0}^2 + {r_2}^2}}{2} \ . \tag{5}$$

There are two solutions: r_{1+} and r_{1-} for a given r_2, this corresponds to contributions from two "gravitational arcs" in the lens plane which add up into an element area of the focal plane: one arc on each side of the lens.

Expressing dr_{1+} and dr_{1-} as a function of dr_2 yields:

$$dr_1 = \frac{dr_2}{2}(1 \pm \frac{r_2}{\sqrt{4\,{r_0}^2 + {r_2}^2}}) \ . \tag{6}$$

Placing r_1 and dr_1 into eq.(3) and adding the two contributions gives:

$$I(r_2) = I_0 \frac{r_1 dr_1}{r_2 dr_2} = \frac{\left(r_2 + \sqrt{4\,{r_0}^2 + {r_2}^2}\right)^2}{4\,r_2\sqrt{4\,{r_0}^2 + {r_2}^2}} + \frac{\left(r_2 + \sqrt{4\,{r_0}^2 + {r_2}^2}\right)^2}{4\,r_2\sqrt{4\,{r_0}^2 + {r_2}^2}} \tag{7}$$

which, when considering $r_2 \ll r_0$ simplifies to the approximation:

$$I(r_2) = I_0 \frac{r_0}{r_2} \ . \tag{8}$$

We can derive a normalized "geometrical" PSF, which can be expressed in Cartesian coordinates: $x_2 = r_2 \cos\alpha$, $y_2 = r_2 \sin\alpha$ and vector $\mathbf{x_2} = (x_2, y_2)$:

$$PSF_{geom}(\mathbf{x_2}) = \frac{r_0}{|\mathbf{x_2}|} \tag{9}$$

This expression, being derived from geometrical hypotheses, tends to infinity at $\mathbf{x} = \mathbf{0}$. This divergence is suppressed by diffraction. What causes problems with such a PSF is the divergence of its surface integral for large $\mathbf{x}$. It may impair the *signal/noise* ratio for small scale features on an extended background.

The diffraction limited point spread function of a single ring aperture of radius r_0 and focal f at wavelength λ would be

$$PSF_{ring}(\mathbf{x_2}, \lambda) = J_0 \left(\frac{\pi |\mathbf{x_2}| r_0}{\lambda f} \right) \tag{10}$$

where J_0 is the zero order Bessel function.

As the light from collecting rings of different diameters travels optical paths which differ by much more than the coherence length, they contribute incoherently to the image. To estimate the order of magnitude of the effect of diffraction, one can consider r_0 constant for the center part of the PSF and write:

$$PSF_{diff}(\mathbf{x_2}, \lambda) \simeq J_0 \left(\frac{\pi |\mathbf{x}| r_0}{\lambda f} \right) \otimes \frac{r_0}{|\mathbf{x_2}|} \tag{11}$$

where $\otimes$ represents a 2D convolution operator and PSF_{diff} is the point spread function of a gravitational lens with diffraction. The above approximation is only for the central and peaked part of PSF_{diff}. A more precise expression should be built from the integration over the different contributing arcs in the pupil plane.

For a distant object $O(\mathbf{x}, \lambda)$, the corresponding image $I(\mathbf{x_2}, \lambda)$ in the focal plane of a perfect sphere gravitational lens is:

$$I(\mathbf{x_2}, \lambda) = O(\mathbf{x}, \lambda) \otimes PSF_{diff}(\mathbf{x_2}, \lambda) \tag{12}$$

For the γ-ray domain, at 511 keV for example, the diffraction effects are small. The first zero of $J_0(z)$ at z=2.405 corresponds to 1.3×10^{-7} m in the focal plane and 2.3×10^{-16} arc seconds angularly. In the next section we show that gravitational aberrations have larger effects than the diffraction at short wavelengths, the turnover being in the submillimetric domain. However, the path length aberrations due to the corona plasma are dominant at all wavelengths longer than the visible or close IR domain.

4 Aberrations

The perturbations of the gravitational potential change the PSF. We will not give expressions for the aberrations, but derive from simple models some upper limits in angular resolution and radiation amplification.

The mass of planets perturb the deflection angles. Furthermore, the sun is not a perfect sphere, due to its rotation and seismic activity.

4.1 Effect of a planet

To first order, the mass of a planet causes a deviation of the caustic. In the focal plane related to impact parameter r_o, the image translation is:

$$\mathbf{x_2} = r_o \frac{m_p r_o}{m_\odot r_p \sin i} \frac{\mathbf{r_p}}{r_p} \tag{13}$$

where vector $\mathbf{r_p}$ corresponds to the heliocentric position of the planet, r_p being its modulus, i the angle between r_p and the line of sight. m_p and $m_\odot$ are respectively the mass of the planet and of the sun.

In addition to translation, aberrations arise. Let's consider two points on a ring of radius r_0 in the pupil plane: the intersections of that ring with a plane containing the optical axis and the center of the planet. Due to the mass of the planet, the deviation angles at those two points differ:

$$\Delta\theta_a = \frac{4Gm_p}{(r_p - r_0)c^2} \text{ and } \Delta\theta_b = \frac{4Gm_p}{(r_p + r_0)c^2} \tag{14}$$

the resulting beams reach the focal plane at a distance $\Delta\mathbf{x}$ from each other :

$$\Delta\mathbf{x_2} = \frac{2r_0^3}{(r_p \sin i)^2} \frac{m_p}{m_\odot} \frac{\mathbf{r_p}}{r_p} . \tag{15}$$

For two other beams in an axial plane perpendicular to the previous one, the deviation angles are equal and $\Delta\mathbf{x_2} = 0$. When considering the whole "collecting ring", the resulting aberration is of elongation $\Delta\mathbf{x_2}$.

Jupiter dominates the other planets for its effect on image displacement and aberration: respectively 1573 m and 6.5 m for a $r_0 = 1.15$ solar radius impact parameter ($f = 724$ AU). Venus causes the second largest displacement and aberration: respectively 29 and 0.8 m. For this upper limit of aberrations, we have considered the cases where the heliocentric angle between the planet and the target $i = 30°$. The best possible case ($i = 90°$) would correspond to aberrations four times smaller.

4.2 Effect of the non sphericity of the sun

The oblateness of the sun is $\Delta r/r_\odot \simeq 1.0\ \ 10^{-5}$ (Stix, 2002) where $r_\odot$ is the solar photosphere radius. To give an upper limit to the resulting aberrations, we consider the rotation axis of the sun perpendicular to the optical axis. We also consider the sun as having a uniform density. This yields a very crude upper limit, as the mass repartition in the sun is strongly offset towards the

smaller values of $r_\odot$, and the oblateness Δr of an equipotential mass $m_\odot$ of mean diameter $r_\odot$ in rotation at ω is given by

$$\Delta r = \frac{\omega^2 r_\odot^4}{2Gm_\odot}$$

We model the gravitational potential in a way similar to modeling the electric potential of a polarized atom: the sun's oblate mass is approximated by two spheres of half the density, their centers being offset by $4\Delta r$. We then consider two perpendicular planes: the equatorial plane and a polar plane, both containing the optical axis.

As $\Delta r << r_\odot$, the oblateness has a negligible effect for beams in the polar plane and we get $\theta_{pol} \simeq \frac{4Gm_\odot}{r_0 c^2}$, whereas in the equatorial plane we have:

$$\theta_{eq} = \frac{4Gm_\odot}{2c^2} \quad \frac{2r_0}{r_0^2 - 4\Delta r^2} \quad .$$

The corresponding size of the aberration in the focal plane is given by:

$$\Delta x = f(2\theta_{eq} - 2\theta_{pol}) = r_0 \frac{8\Delta r^2 / r_0^2}{1 - 4\Delta r^2 / r_0^2} \quad ,$$

which, when considering $\Delta r << r_0$ simplifies into:

$$\Delta x = \frac{8\Delta r^2}{r_0} \quad . \tag{16}$$

This corresponds to an aberration of 0.37 m for a $r_0 = 1.15$ solar radius impact parameter – comparable to, but smaller than, the planetary perturbations.

The actual shape of the PSF due to planets positions and the oblateness of the sun is stable in time and can be modeled, so a matched deconvolution of the images in the focal plane could be performed, improving the resolution. However, other aberrations may arise from less predictable phenomena.

4.3 Other causes of gravitational aberrations

The gravitational potential is affected by the density variations from helioseismic activity. To estimate these perturbations, we based our assumptions on data in "Astrophysical Quantities" (Cox & Allen, 1999) and "The Sun" (Stix, 2002).

We find an upper limit for the aberrations of 2.4 meters at the focal plane corresponding to $r_0 = 1.1$ solar radius, considering the contribution

	X band	K band	millimedtric	10 microns	1 micron	visible	1,2 keV	511 keV
frequency in Hz	8,00E+09	3,20E+10						
wavelength in m			1,0E-03	1,0E-05	1,0E-06	5,0E-07		
Energy in eV							1,24E+03	5,11E+05
déviation for R0= 1.2 solar radii	5,0E-4	3,1E-5	3,6E-7	3,6E-11	3,6E-13	9,0E-14	3,6E-19	2,1E-24
déviation at focus (m)	5,4E+10	3,4E+9	3,9E+7	3,9E+3	3,9E+1	9,7E+0	3,9E-5	2,3E-10

Figure 3: Angular and linear deviations of electromagnetic radiations by the solar corona plasma at 1.2 solar radii for different wavelengths.

from the whole spectrum of radial "p" modes. This upper limit is crudely overestimated. We have not been able to derive before the deadline for this paper a robust expression of these gravitational perturbations. This should be investigated by people more competent in solar physics. The perturbations of the gravitational field are generally neglected in the literature for the equations that describe the pulsation modes of the sun.

4.4 Aberrations due to the corona plasma

The refractive index of the solar corona plasma has been measured during several experiments made to test the validity of general relativity using the deflection of quasar sources angularly approaching the sun. The refraction effect has been probed in the radio domain, and its dependance over wavelength in λ^2 has been published by Anderson et al. (2004) for solar distances from $r_0 = 1.2$ to 5 solar radii in the X and K bands (8 and 32 GHz, respectively). The deviations deduced from these data at shorter wavelengths are given in the table in Figure 3.

This table is based on an averaged value of the coronal plasma index, considered isotropic around the sun and constant in time. Such a model causes a mere defocus, which should not affect the size nor the position of the caustic line, except for the distance of the closest focal plane. This would not induce aberrations. What causes aberrations is the non centro-symmetry of the solar corona index. In a conservative estimate of aberrations made here, we consider the upper limit of the index variations being as large as the average value.

Considering this upper limit, the aberrations caused by corona index become smaller than those caused by planets (10 meters) at wavelengths shorter or equal to those of the visible domain. They should be negligible at high energies.

4.5 Contribution of the direct solar light

In the visible and at shorter wavelengths, the size of the aberration patch leads to amplification factors of 6.1×10^7(19.5 magnitudes) in the case of an unresolved stellar black hole accretion disk, and 5.6×10^5(14.4 mag) in the case of the galaxy center accretion disk, which has an extended image : 180 km in the focal plane.

The sun at 500 AU from the focal plane is brighter in the visible (V = −13) and UV than the amplified targets, and exactly aligned with them, limiting observations to the γ domain. However, for the UV and softer domains the contribution from the sun can be filtered out by a mask in the focal instrument, letting through the light from the imaged Einstein ring and blocking the central image of the sun. Such a simple device could reduce the apparent brightness of the sun by 5 magnitudes or more.

5 Deconvolution

In contrast to a standard optical instrument, the PSF of a gravitational lens does not converge when integrated over the image plane. For a given point, the contribution of an illuminated field through this PSF integrates as:

$$I(0) = \int_r \int_\theta O(r_2, \theta) \frac{1}{r_2} r_2 dr_2 d\theta = \iint O(r_2, \theta) dr_2 d\theta \tag{17}$$

where $O(r_2, theta)$ is the field illumination expressed in radial coordinates. Due to the convolution by that PSF, sources in the close vicinity (less than a few milli arc seconds) and extended objects will contribute to a continuous background. We have simulated the convolution of a modeled extended object (an accretion disk around a black hole) by the PSF of a gravitational lens. Figures 5–7 show the model object, its convolution with the PSF (photon noise is added corresponding to 100 photons/pixel at the brightest point), and the result of a simple de-convolution regularized by a low-pass filtering in spatial frequencies. In this simulation, the aberrations have been neglected, as the aberration size is smaller than the pixel size.

6 Prospective mission, object acquisition and image field scanning

One of the main challenges for this type of observation is to send a probe at more than 550 UA from the sun. This could be achievable by sling shots

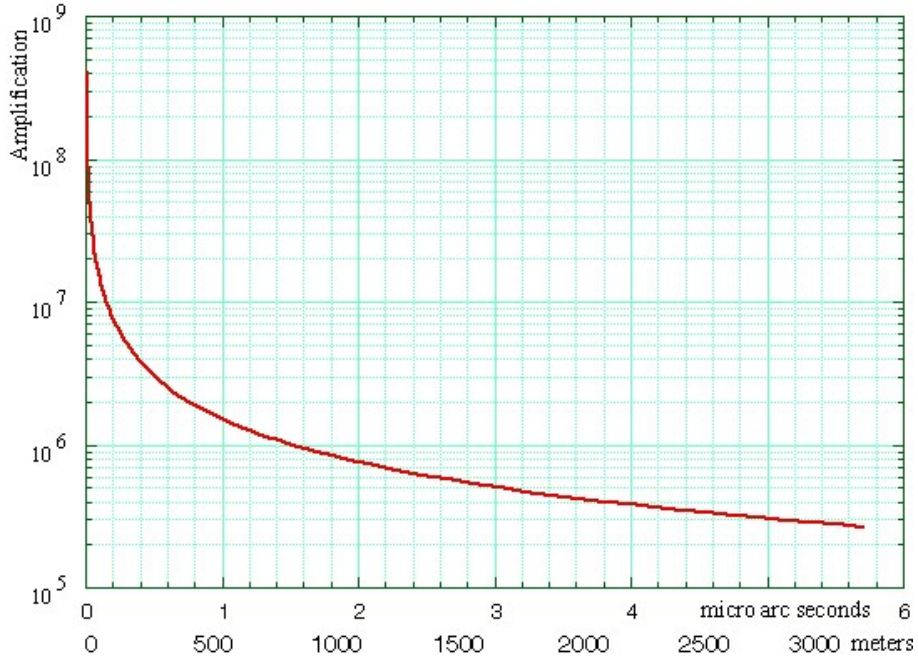

Figure 4: Point Spread Function in a focal plane at 724 astronomical units from the sun. The horizontal axis shows the offset from the center of the field in micro arc seconds and the correspondence distance in meters. The vertical axis plots the light intensification factor, limited to 4.4×10^8 as the aberrations caused by the planets spread the light over a 2 meter diameter patch.

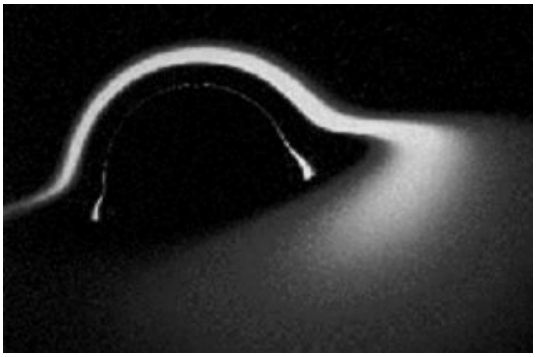

Figure 5: An accretion disk around a black hole used as a model object for convolution by the psf of a gravitational lens. Image from numerical simulations by J-P. Luminet.

.

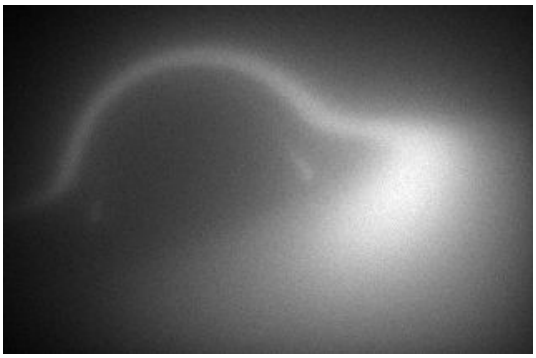

Figure 6: Image in the focal plane, obtained after convolution by the PSF. Photon noise is added, corresponding to 100 photons per pixel.

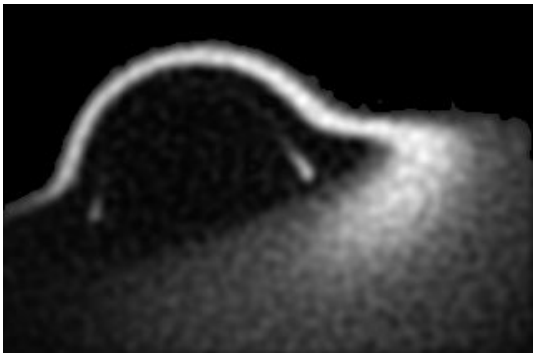

Figure 7: Deconvolved image using the gravitational PSF. Low-pass filtering in spatial frequencies is applied.

Astrophysical targets

Only one possible field for a given mission

Mission parameters	Galactic center	Stellar black hole	AGN
Accr disk inner radius	$2.2\ 10^{10}$ m	$1.6\ 10^{4}$ m	$6\ 10^{10}$ m
distance	8.5 k Pc	200 Pc	20 M Pc
Estimated raw ph s^{-1} m^{-2}	100	10^{5}	0.2
Image size at focal plane	20 km	0.63 m	23 m
Detector area	1 m^2	0,01 m^2	0,01 m^2
Photons / s on detector	$4.7\ 10^{3}$ ph s^{-1}	$3.8\ 10^{11}$ ph s^{-1}	$3.6\ 10^{6}$ ph s^{-1}
Image resolution elements	7000 x 7000	1	12 x 12

Figure 8: Possible targets for a gravitational focussing X or γ mission.

around inner planets and/or by ionic thrusters in the accelerated first part of the trajectory, where solar energy is available at a sufficient level.

The probe will not have to slow down or stop at a given focal plane: it can travel along the caustic at unreduced speed, increasing its distance to the sun by 100 or 200 AU during the time of the observation mission. In addition to this constant motion, several scans of a hundred lines each in a 100×100 km area in the focal plane can be performed by the use of slow motion thrusters, in order to sample a 0.1 mas field, yielding a 100×10000 pixel image.

One of the disadvantages of the PSF: its very extended wings, will turn out to be of some help for the acquisition of a target object as its coordinates will not be known with enough precision to locate it on the detector directly.

There would be no possibility to change the target once the observation mission is started. Three possible targets are presented in the table in Figure 8: Sagitarius A*, a stellar gamma source as Cyg X 1, and an AGN.

7 Conclusion

Being independent of the type of radiation and thus perfectly achromatic for mass-less particles, the main interest of gravitational focussing is for ra-

diations difficult to focus otherwise, such as X and gamma rays, and perhaps gravitational waves (Nemiroff 2005). Neutrinos will be also focussed, at shorter distances from the sun.

We have investigated the possible causes of aberrations. This paper is a coarse approach of the problem, and there is room for a lot of improvement. For example, none of the authors of this paper are specialists in helioseismology and its consequences on focussing deserve more investigation.

The main drawbacks of this technique are the large distances required for reaching the closest focal points, and the "single field" nature of a space mission to any of those points. The image processing required to extract all the information from the foggy "raw images" will give work to image processing scientists, but these raw images seem usable, and the available deconvolution techniques should improve them significantly.

The advantages are very attractive : a perfectly achromatic instrument giving amplifications of 10^8 or more for radiations hard to focus otherwise, and nano arc second angular resolutions.

References

[1] John D. Anderson, Eunice L. Lau, Giacomo Giampieri - "Improved Test of General Relativity with Radio Doppler Data from the Cassini Spacecraft", 22nd Texas Symposium on Relativistic Astrophysics 15 December 2004

[2] Cox N. Allen C. 1999 "Astrophysical Quantities" 4th ed. (Springer) p.147.

[3] Dyson, F.W., Eddington, A.S., and Davidson C.R., *M.N.R.A.S.* 1919. "A determination of the deflection of light by the sun's gravitational field from observations made at the total eclipse of May 29, 1919"

[4] Einstein, A. *Science* , **84** p.506, 1936. "Lens-like Action of a Star by the Deviation of Light in the Gravitational Field"

[5] Fomalont, E. B. and Sramek, R. A. *Ap.J.*, **199** pp.749-755, 1975.

[6] Macone C. "The Sun as a Gravitational Lens: Proposed Space Missions", (IPI Press: www.ipipress.com), 2002.

[7] Nemiroff R.J.*Ap.J.*, **628**, part 1, pp.1081-1085, 2005.

[8] Paczynski, B. *An. Rev. Astro. Ap*, **34** p. 419, 1996.

[9] Michel Stix : "The Sun. An introduction", Second edition 2002, *A & A Library*, Springer ISBN 0941 7834

[10] Zwicky, F. *Phys. Rev* , **51** , p.290 & 679, 1937.